A second-generation reactive empirical bond order (REBO) potential energy expression for hydrocarbons

To cite this article: Donald W Brenner *et al* 2002 *J. Phys.: Condens. Matter* **14** 783

View the article online for updates and enhancements.

A second-generation reactive empirical bond order (REBO) potential energy expression for hydrocarbons

Donald W Brenner[1]**, Olga A Shenderova**[1]**, Judith A Harrison**[2]**,
Steven J Stuart**[3]**, Boris Ni**[4] **and Susan B Sinnott**[4]

[1] Department of Materials Science and Engineering, North Carolina State University, Raleigh, NC 27695-7907, USA
[2] Department of Chemistry, United States Naval Academy, Annapolis, MD 21402, USA
[3] Department of Chemistry, Clemson University, Clemson, SC 29634-0973, USA
[4] Department of Materials Science and Engineering, University of Florida, Gainesville, FL 32611-6400, USA

E-mail: brenner@eos.ncsu.edu

Abstract
A second-generation potential energy function for solid carbon and hydrocarbon molecules that is based on an empirical bond order formalism is presented. This potential allows for covalent bond breaking and forming with associated changes in atomic hybridization within a classical potential, producing a powerful method for modelling complex chemistry in large many-atom systems. This revised potential contains improved analytic functions and an extended database relative to an earlier version (Brenner D W 1990 *Phys. Rev.* B **42** 9458). These lead to a significantly better description of bond energies, lengths, and force constants for hydrocarbon molecules, as well as elastic properties, interstitial defect energies, and surface energies for diamond.

1. Introduction

The reliability of atomistic Monte Carlo and molecular dynamics simulations—techniques that have impacted on areas ranging from drug design to crystal growth—depends on the use of appropriate interatomic energies and forces. These interactions are generally described using either analytic potential energy expressions or semi-empirical electronic structure methods, or obtained from a total-energy first-principles calculation. While the latter approach is not subject to errors that can arise from the assumed functional forms and parameter fitting usually required in the first two methods, there remain clear advantages to classical potentials for large systems and long simulation times.

One of us introduced a classical potential energy expression for carbon and hydrocarbon molecules that allows for bond making and breaking with appropriate changes in atomic hybridization [1]. Although originally developed to model the chemical vapour deposition of diamond films, this expression has found use in simulating a wide range of other structures and chemical processes. These include reactive surface and cluster dynamics [2–7], fullerene formation and properties [8–11], properties of carbon melts [12, 13], and processes associated with nanoindentation and friction [14–26].

In this paper, the details of an improved 'second-generation' form of this hydrocarbon potential energy expression are described. This revised potential includes both modified analytic functions for the intramolecular interactions and an expanded fitting database. The revised expression has already been used to model a wide variety of processes, including reactive surface and cluster dynamics [27–34], carbon nanotube properties [35–44], polycrystalline diamond structure [45–47], brittle fracture dynamics [48], and processes associated with nanoindentation [49].

As before [1], the goal of this work is to develop a potential energy expression that: (1) reproduces, with the same potential energy expression, bonding characteristics for solid carbon as well as various hydrocarbon molecules in the fitting database; (2) yields binding energies and bond lengths that are reasonably transferable to systems not included in the fitting database; (3) allows for covalent bond breaking and forming with appropriate changes in atomic hybridization; and (4) is not computationally intensive. The new function yields a much improved description of bond energies, lengths, and especially force constants for carbon–carbon bonds as compared to the earlier effort [1]. This has produced an improved fit to the elastic properties of diamond and graphite, which in turn yield better predictions for the energies of several surface reconstructions and interstitial defects. Forces associated with rotation about dihedral angles for carbon–carbon double bonds as well as angular interactions associated with hydrogen centres have also been modelled which were not included in the original effort.

This paper begins in the next section with a brief discussion of the Abell–Tersoff bond order formalism that is the basis of the potential described here. This form is not based on a traditional many-body expansion of potential energy in bond lengths and angles [50]; instead, a parametrized bond order function is used to introduce many-body effects and chemical bonding into a pair potential. The next section gives the analytic functions for the empirical bond order and pair potentials used to describe carbon. It also includes a detailed discussion of the fitting procedure. The latter information is important both so that the strengths and limitations of this expression can be recognized, and so that a comparable fitting scheme can be developed by others who may want to parametrize a similar function for other systems. This is followed by descriptions of the function used to model H_3 and hydrocarbon molecules, again including details of the fitting procedure. Predictions given by the potential for a wide range of systems, including solid-state, surface, and molecular properties, are then compared to either experimental values or high-quality total-energy calculations.

2. Abell–Tersoff bond order potentials

The general analytic form used for the intramolecular potential energy was originally derived by Abell from chemical pseudopotential theory [51]. Beginning with a local basis of unperturbed atomic orbitals, Abell showed that chemical binding energy E_b can be simply written as a sum over nearest neighbours in the form

$$E_b = \sum_i \sum_{j(>i)} [V^R(r_{ij}) - b_{ij} V^A(r_{ij})]. \tag{1}$$

The functions $V^R(r)$ and $V^A(r)$ are pair-additive interactions that represent all interatomic repulsions (core–core, etc) and attraction from valence electrons, respectively. The quantity r_{ij} is the distance between pairs of nearest-neighbour atoms i and j, and b_{ij} is a bond order between atoms i and j that is derivable from Huckel or similar level electronic structure theory.

Abell argued that local coordination N is the primary quantity controlling the value of the bond order, and using a Bethe lattice derived the simple expression for regular structures

$$b \propto (N)^{-1/2}. \tag{2}$$

With Morse-type pair interactions, equations (1) and (2) yield an energy versus volume relationship similar to a universal binding energy curve while at the same time producing systems preferring open or close-packed structures depending on the ratio of the slopes of the repulsive to attractive pair terms. Furthermore, the form predicts an increase in bond length and a decrease in individual bond energies as coordination increases. This is consistent with well-established chemical trends. The simplified bond order expression equation (2) can also be derived from the second-moment approximation relating local coordination to the broadening of orbital energies [52].

Recognizing the utility of Abell's approach, Tersoff introduced analytic parametrized forms for the bond order that were able to describe bonding in ambient and high-pressure phases of group IV elements as well as a number of surface and solid-state defect energies in these elements and their alloys [53–56]. The value of the bond order was assumed to depend both on the local coordination and on bond angles. The latter is required to stabilize open lattices against shear distortion, and to model elastic properties and defect energies with reasonable accuracy.

In our subsequent work, the use of Tersoff's solid-state empirical bond order scheme was tested for molecular systems by fitting similar expressions to molecular mono-elemental systems of hydrogen and oxygen [57] as well as model reactive molecular solids [58,59]. After establishing that this approach can be applied to both solid-state and molecular systems [57–59], the first-generation form of this potential for hydrocarbon molecules and solid carbon was developed [1]. A variety of similar empirical bond order expressions have been developed since the Tersoff form was introduced. These include improved forms for modelling silicon [60–63], potentials for other covalently bonded systems such as GaAs [63] and SiN [64], and forms for molecular structures that include hydrogen [63–69]. There has also been recent progress in incorporating weak non-bonded interactions within the bond order formalism [70,71].

Pettifor and co-workers [72–74] have gone beyond the Tersoff empirical bond order form by deriving an analytic form directly from a tight-binding Hamiltonian using the moments theorem. Their most recent bond order expression explicitly includes pi and sigma bonding with associated angular interactions.

3. Analytic bond order form

The general Abell–Tersoff form equation (1) is used for the total potential energy. Following the earlier hydrocarbon bonding expression [1], the empirical bond order function used here is written as a sum of terms:

$$\overline{b}_{ij} = \tfrac{1}{2}[b_{ij}^{\sigma-\pi} + b_{ji}^{\sigma-\pi}] + b_{ij}^{\pi}. \tag{3}$$

Values for the functions $b_{ij}^{\sigma-\pi}$ and $b_{jj}^{\sigma-\pi}$ depend on the local coordination and bond angles for atoms i and j, respectively. The function b_{ij}^{π} is further written as a sum of two terms:

$$b_{ij}^{\pi} = \Pi_{ij}^{\mathrm{RC}} + b_{ij}^{\mathrm{DH}}. \tag{4}$$

The value of the first term Π_{ij}^{RC} depends on whether a bond between atoms i and j has radical character and is part of a conjugated system. The value of the second term b_{ij}^{DH} depends on the dihedral angle for carbon–carbon double bonds. This expression combined with equation (1) is used to define the binding energy due to covalent bonding of any collection of hydrogen and carbon atoms. No predetermined atomic hybridizations are assumed as in traditional valence-force fields; instead, atomic bonding is determined strictly from local bonding neighbours and non-local conjugation as defined below. Because the local bonding environment determines the effective interatomic interactions, and not the other way around, the influence of atomic rehybridization on the binding energy can be modelled as covalent bonds break and reform within a classical potential.

The specific analytic forms for the pair terms and bond order function given below are somewhat complicated, and the number of parameters needed is large to accurately model carbon bonding for the wide range of atomic hybridizations considered. To simplify the fitting procedure, a two-step process was developed. In the first step, functional forms and parameters for the pair terms in equation (1) and discrete values of the empirical bond order function were obtained. For carbon–carbon bonds, the data used to fit the potential in this step consist of triple-, double-, and single-bond energies, lengths and force constants, as well as bond energies for solid-state simple cubic (SC) and face-centred cubic (FCC) lattices. In the second step of the fitting procedure, parameters in the bond order function are fitted to the discrete values of the bond order determined in the first step, as well as additional properties such as vacancy formation energies and barriers for rotation about carbon–carbon double bonds. In the latter step, direct correlations between individual parameters and physical properties are attempted within physically motivated choices for the functional forms.

A similar fitting scheme is used for hydrogen, where the fitting properties include the H_2 binding energy, bond length, and vibrational frequency as well as information related to the $H + H_2$ reactive potential energy surface. With interactions defined for systems of pure carbon and hydrogen, determining a potential energy function for hydrocarbon molecules involves defining relatively small 'correction' terms to the bond order expression plus additional parameters related to energy barriers for a number of hydrogen exchange reactions. Details of the functional forms and fitting of these systems are given below.

4. Carbon bonding

Following Tersoff [53–56], the first-generation hydrocarbon expression used Morse-type terms for the pair interactions in equation (1) [1]. However, it was determined that this form is too restrictive to simultaneously fit equilibrium distances, energies, and force constants for carbon–carbon bonds. This form has the further disadvantage that both terms go to finite values as the distance between atoms decreases, limiting the possibility of modelling processes involving energetic atomic collisions. In this second-generation potential, the forms

$$V^R(r) = f^c(r)(1 + Q/r)A\mathrm{e}^{-\alpha r} \tag{5}$$

and

$$V^A(r) = f^c(r) \sum_{n=1,3} B_n \mathrm{e}^{-\beta_n r} \tag{6}$$

are used for the pair terms. The subscript n refers to the sum in equation (6), and r is the scalar distance between atoms. The screened Coulomb function used for the repulsive pair interaction (equation (5)) goes to infinity as interatomic distances approach zero, and the attractive term (equation (6)) has sufficient flexibility to simultaneously fit the bond properties that could not be fitted with the Morse-type terms used previously. The function $f^c(r)$ limits the range of

Table 1. Data used in the fitting scheme.

Species	ΔH (eV)[a]	Zero-point energy (eV)[b]	Atomization energy (eV)[c]	Bond energy (eV)	Bond distance (Å)	Force constant (10^5 dyn cm^{-1})
Diamond	—	—	7.36[d]	3.68	1.54	4.73[e]
Graphite	—	—	7.40[d]	4.93	1.42	6.98[f]
SC	—	—	4.70[d]	1.57	1.93[d]	
FCC	—	—	2.86[d]	0.46	2.18[d]	
Ethyne	2.356	0.701	17.57	8.51	1.20	16.00[g]
Ethene	0.629	1.339	24.41	6.30	1.33	9.56[f]
Ethane	−0.717	1.955	30.84	3.69	1.54	4.79[f]
Cyclohexane	−0.868	4.496	76.45	3.69	1.54	4.79[f]
Benzene	1.041	2.677	59.29	5.36	1.39	7.85[f]
C–H bonds	—	—	—	4.526	1.09	—

[a] From [86].
[b] Calculated assuming harmonic interactions.
[c] Calculated assuming $\Delta H_{carbon} = 7.37$ eV, $\Delta H_{hydrogen} = 2.239$ eV.
[d] From [87].
[e] Calculated from the bulk modulus of diamond $= 4.4 \times 10^{12}$ dyn cm^{-2}.
[f] From equation (7) ($a = 4.99682 \times 10^5$ Å^3 dyn cm^{-1}, $b = 0.52554$ Å).
[g] From [88].

the covalent interactions. The parameter fitting for carbon discussed below assumes a value of one for $f^c(r)$ for nearest neighbours and zero for all other interatomic distances. This choice is discussed at the end of this section.

The database used for fitting the parameters in the pair interactions and the values of the bond order b_{CC} consists of equilibrium distances, energies, and stretching force constants for single (from diamond), conjugated double (from graphite), full double (from ethene), and triple (from ethyne) bonds. Values for these properties were determined in the following way. First, minimum-energy distances were taken from standard literature references; these are given in table 1. Values for the force constants for the complete range of atomic hybridizations considered here were then obtained from the Badger rule expression

$$K = a(r_e - b)^{-3} \tag{7}$$

where K is the force constant, r_e is the minimum-energy bond distance, and a and b are adjustable parameters. Values for the latter two parameters were determined from the force constants and minimum-energy distances for carbon–carbon single and triple bonds. These are given in table 1. Equation (7) was then used to determine a continuous range of force constants, including the remaining values given in table 1.

Existing bond-additive values for determining molecular heats of formation of hydrocarbons generally include zero-point energies. Therefore for this classical potential a new set of values without zero-point energies had to be determined. To derive these, heats of formation and zero-point energies for the molecules C_2H_2, C_2H_4, C_2H_6, c-C_6H_{12}, and c-C_6H_6 (benzene) were used to determine molecular atomization energies. These values are given in table 1. Assuming a constant value for the carbon–hydrogen bond energy in each of these molecules, these atomization energies provide a complete set of data from which bond-additive energies for molecular carbon–carbon single, double, conjugated double and triple bonds, as well as the carbon–hydrogen bond can be derived. The resulting bond contributions to the atomization energy are given in table 1.

To reduce the number of variables needed to fit the pair terms, the procedure used initial guesses for the variables A_{CC}, Q_{CC}, α_{CC}, B_{CC1}, B_{CC2}, β_{CC1}, and β_{CC2}. Values for B$_{CC3}$ and β_{CC3}
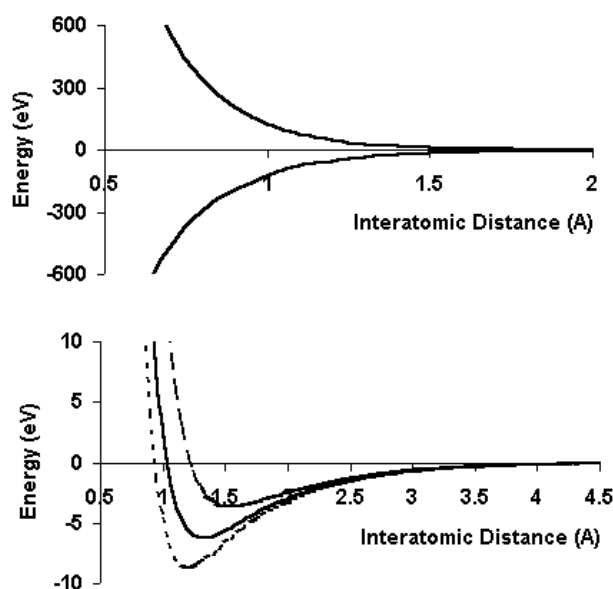
Figure 1. Plots of the pair potentials (5) and (6) obtained using the parameters in table 1. Top: the attractive and repulsive pair terms as a function of interatomic distance. Bottom: pair terms for triple bonds (dotted curve), double bonds (solid curve), and single bonds (dashed curve) obtained by multiplying the attractive pair term by the appropriate bond order value and adding it to the repulsive pair term.

Table 2. Parameters for the carbon–carbon pair terms, equations (5) and (20).

$B_1 = 12\,388.791\,977\,98$ eV	$\beta_1 = 4.720\,452\,3127$ Å^{-1}	$Q = 0.313\,460\,296\,0833$ Å
$B_2 = 17.567\,406\,465\,09$ eV	$\beta_2 = 1.433\,213\,2499$ Å^{-1}	$A = 10\,953.544\,162\,170$ eV
$B_3 = 30.714\,932\,080\,65$ eV	$\beta_3 = 1.382\,691\,2506$ Å^{-1}	$\alpha = 4.746\,539\,060\,6595$ Å^{-1}
$D_{\min} = 1.7$	$D_{\max} = 2.0$	

were determined by solving the sum of equations (5) and (6) for the single-bond equilibrium distance and energy. The value of the bond order b_{CC} for single bonds was then considered B_{CC3}, and all three of the B_{CCn} were normalized by this value. Each of the bond orders for the remaining three equilibrium bond lengths were then determined by setting the derivative of the sum of equations (5) and (6) to zero at each distance. The values for the remaining bond energies and force constants were then calculated and a least-squares sum was computed from the values in table 1. Finally, the variables A_{CC}, Q_{CC}, α_{CC}, B_{CC1}, B_{CC2}, β_{CC1}, and β_{CC2} were readjusted using a standard fitting routine. These steps were repeated until the least-squares sum was minimized. Values of the bond order for coordinations of six and twelve were then determined by calculating the values that give a minimum bond energy that corresponds to the SC and FCC lattices, respectively. At the end of this process, each of the b_{CC} and B_{CCn} was normalized such that for a bond order of one, the bond energy is equal to that appropriate for diatomic carbon. The final parameter values obtained in this way are given in table 2.

Plotted at the top of figure 1 are the repulsive and attractive pair terms (equations (5) and (6), respectively) determined as described above as a function of interatomic distance. Plotted at the bottom of figure 1 are curves corresponding to molecular triple, double, and single bonds. These were obtained by multiplying the attractive pair term by the appropriate
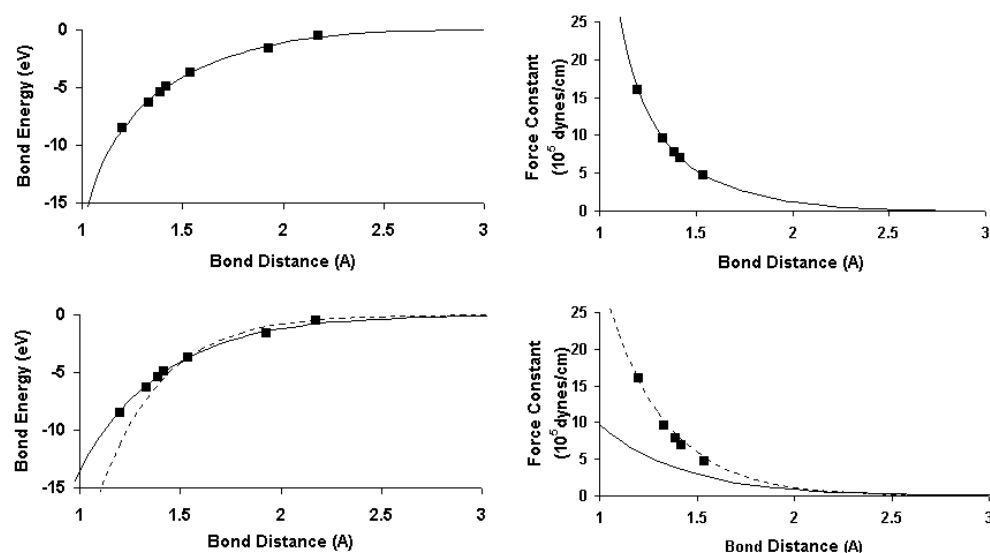
Figure 2. Plots of pair term properties. Top left and top right panels: plots of bond energy and force constant, respectively, versus bond distance for the pair terms developed here. Bottom panels: corresponding properties for potential I (solid curves) and potential II (dotted curves) in [1].

value of the bond order and adding it to the repulsive pair term. Plotted in the top left and top right panels of figure 2 are bond energy and force constant, respectively, as a function of equilibrium bond distance for the pair terms in figure 1. For reference, the bond energy and force constant as a function of equilibrium distance are plotted in the bottom two panels of figure 2 for potential 1 and potential 2 of [1]. These two potentials assumed Morse-type functions for the pair terms. The fitting data from table 1 are indicated by the squares in each plot. It is clear that the Morse functions used in the previous-generation hydrocarbon potentials are unable to describe bond energies, distances, and force constants simultaneously for carbon–carbon bonds. On the other hand, the functions developed here are able to describe each of these properties relatively accurately. It is clear that when carefully chosen pair terms are used, this formalism—pair terms coupled to a bond order—is capable of describing bonding properties with relatively high accuracy over a large range of values. Moreover, it is encouraging that equilibrium bond lengths for SC and FCC lattices are very well predicted by these functions despite not fitting the pair terms to these large bonding distances.

Analytic forms for each term in equation (2) are fitted to both the discrete values of the bond orders determined above, and to other properties of solid-state and molecular carbon as described below. Following the earlier hydrocarbon effort [1], the first term in equation (3) is given as

$$b_{ij}^{\sigma-\pi} = \left[1 + \sum_{k\,(\neq i,j)} f_{ik}^c(r_{ik})G(\cos(\theta_{ijk}))e^{\lambda_{ijk}} + P_{ij}(N_i^C, N_i^H)\right]^{-1/2}. \tag{8}$$

As in equations (5) and (6), the subscripts refer to the atom identity, and the function $f^c(r)$ ensures that the interactions include nearest neighbours only. The function P represents a bicubic spline and the quantities N_i^C and N_i^H represent the number of carbon and hydrogen atoms, respectively, that are neighbours of atom i. These are defined by the sums

$$N_i^C = \sum_{k\,(\neq i, j)}^{\text{carbon atoms}} f_{ik}^c(r_{ik}) \tag{9}$$

and

$$N_i^H = \sum_{l\,(\neq i, j)}^{\text{hydrogen atoms}} f_{il}^c(r_{il}). \tag{10}$$

For solid-state carbon, values of λ and the function P are taken to be zero (with one exception described below). The latter function can be envisioned as 'corrections' to the solid-state analytic bond order function that are needed to accurately model molecular bond energies. An identical expression is given for $b_{ji}^{\sigma-\pi}$ by swapping the i- and j-indices in equation (8).

The function $G_C(\cos(\theta_{jik}))$ in equation (8) modulates the contribution that each nearest neighbour makes to the empirical bond order according to the cosine of the angle of the bonds between atoms i and k and atoms i and j. This function was determined as follows. The diamond lattice and graphitic sheets contain only one angle each, $109.47°$ and $120°$, respectively. Equation (8), together with the values of b_{CC} in figure 2, top left panel, yields values for $G_C(\cos(\theta))$ at each of these angles. The energy difference between the linear C_3 molecule and one bent at an angle of $120°$ (as given by a density functional calculation [75]) was then used to find a value for $G_C(\cos(\theta = 180°))$. Because in a SC lattice the bond angles among nearest neighbours are $90°$ and $180°$, the value of $G_C(\cos(\theta = 180°))$ combined with the value of the bond order for the SC lattice was used to find a value of $G_C(\cos(\theta = 90°))$. Finally, the FCC lattice contains angles of $60°$, $120°$, $180°$, and $90°$. A value for $G_C(\cos(\theta = 60°))$ can therefore be determined from the values of $G_C(\cos(\theta))$ determined above and b_{CC} for the FCC lattice. The values of $G_C(\cos(\theta))$ determined in this way are indicated by the squares in figure 3. This approach to fitting an angular interaction does not rely on an expansion about an equilibrium bond angle. Instead, a single function is used for all atomic hybridizations. This allows the influence of bond angles on the potential energy to change in a continuous fashion as chemical reactions progress. Moreover, it is encouraging that fitting $G_C(\cos(\theta))$ in this way yields values that become monotonically smaller as the angle increases. This behaviour can be interpreted as being due to valence shell electron pair repulsions, a standard concept used for rationalizing shapes of small molecules.

To complete an analytic form for the angular function $G_C(\cos(\theta))$, sixth-order polynomial splines in $\cos(\theta)$ were used in three regions of bond angle θ, $0° < \theta < 109.47°$, $109.47° < \theta < 120°$, and $120° < \theta < 180°$. Because there are six spline coefficients, six values of the function or its derivatives are needed in each region to define the angular function. For values of the angle θ between $109.47°$ and $120°$, the polynomial was fitted to the values of $G_C(\cos(\theta))$ at θ equal to $109.47°$ and $120°$ determined above as well as the first and second derivatives of $G(\cos(\theta))$ with respect to $\cos(\theta)$ at these two angles. Values of the second derivatives of $G(\cos(\theta))$ at $109.47°$ and $120°$ were fitted to the elastic constant c_{11} for diamond and the in-plane elastic constant c_{11} for graphite, respectively. The first derivatives were chosen to suppress spurious oscillations in the splines. The information needed to construct this spline is given in table 3.

Two modifications had to be made to the angular function as determined above to complete the polynomial splines. First, it was determined that for the region $120° < \theta < 180°$, a slightly smaller value of $G(\cos(\theta = 180°))$ than that determined above was needed to determine a first derivative that both suppressed spurious oscillations and gave a reasonable value for the bending force constant for ethyne. Therefore a value of -0.01 was used for $G(\cos(\theta = 180°))$, and the binding energy for the molecule C_3 was recovered by adjusting the value of the function $P_{CC}(1, 0)$. The first and second derivatives of $G(\cos(\theta = 180°))$ were
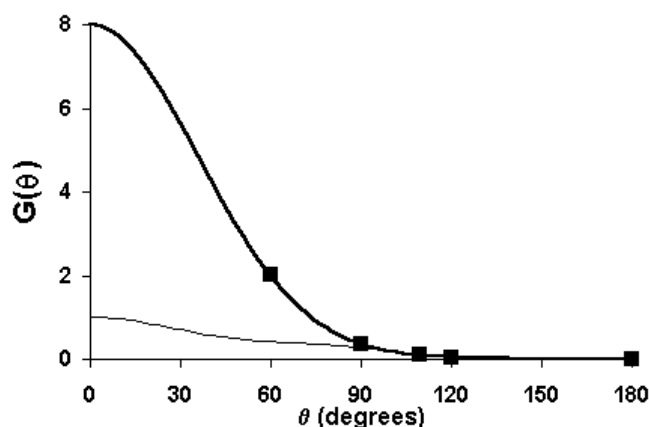
Figure 3. The angular contribution to the bond order equation (8). Squares: fitting data derived from the discrete bond order values. Heavy curve: spline fit to the data. Light curve: modified form for low-coordination structures.

Table 3. Parameters for the angular contribution to the carbon bond order.

θ (rad)	$G(\cos(\theta))$	$dG/d(\cos(\theta))$	$d^2G/d(\cos(\theta))^2$	$\gamma(\theta)$
0	8	—	—	1
$\pi/3$	2.0014	—	—	0.416335
$\pi/2$	0.37545	—	—	0.271856
0.6082π	0.09733	0.40000	1.98000	—
$2\pi/3$	0.05280	0.17000	0.37000	—
π	−0.001	0.10400	0.00000	—

then determined by fitting the ethyne bending mode and by removing spurious oscillations in the spline, respectively. These two derivatives together with the values of the function at the knots are sufficient to determine the spline coefficients. Values for the function and derivatives of $G(\cos(\theta = 180°))$ needed to generate the spline coefficients are reported in table 3.

For angles θ between $0°$ and $109.47°$, the spline was fitted to the value, first derivative, and second derivative of $G_C(\cos(\theta = 109.47°))$, and to values of $G_C(\cos(\theta))$ at θ equal to $90°$, $60°$, and $0°$. The latter value was assigned to yield a smooth function as angles became less than $60°$. Analysis of the energy of small ring hydrocarbons, however, revealed that the values for $G_C(\cos(\theta))$ determined above for θ equal to $90°$ and $60°$ are too large for undercoordinated carbon atoms (they were determined above from eightfold- and twelvefold-coordinated carbon atoms, respectively). To allow for both overcoordinated and undercoordinated atoms, a second spline $\gamma_C(\cos(\theta))$ was determined for angles less than $109.47°$ that was coupled to $G(\cos(\theta))$ through the local coordination. This function retains the value, first derivative, and second derivative at θ equal to $109.47°$ of the original function $G_C(\cos(\theta))$, but has the smaller values at angles of $90°$, $60°$, and $0°$ given in table 3. The revised angular function between $109.47°$ and $0°$ for a carbon atom i is given by

$$g_C = G_C(\cos(\theta)) + Q(N_i^t)[\gamma_C(\cos(\theta)) - G_C(\cos(\theta))] \tag{11}$$

where the function Q is defined by

$$Q_i(N_i^t) = \begin{cases} 1 & N_i^t < 3.2 \\ [1 + \cos(2\pi(N_i^t - 3.2))]/2 & 3.2 < N_i^t < 3.7 \\ 0 & N_i^t > 3.7. \end{cases} \tag{12}$$

The quantity N_i^t is the coordination of atom i given by

$$N_i^t = N_i^C + N_i^H \tag{13}$$

where N_i^C and N_i^H are defined by equations (9) and (10), respectively. Coupling the two spline functions in this way ensures that the overall function is continuous through its second derivative independent of the value of N_i^t. The angular function for N_i^t equal to 3.7 and higher is illustrated in figure 3 by the solid curve. The revised function for N_i^t less than 3.2 is illustrated by the light dashed curve in figure 3.

The term π_{ij}^{RC} in equation (3) represents the influence of radical energetics and π-bond conjugation on the bond energies. As discussed in relation to the first-generation form of this potential [1], this term is necessary to correctly describe radical structures such as the vacancy formation energy in diamond, and to account for non-local conjugation effects such as those that govern the different properties of the carbon–carbon bonds in graphite and benzene. This function is taken as a tricubic spline F:

$$\pi_{ij}^{RC} = F_{ij}(N_i^t, N_j^t, N_{ij}^{conj}) \tag{14}$$

that depends on the total number of neighbours of bonded atoms i and j as defined in equation (13), as well as a function N_{ij}^{conj} that depends on local conjugation.

To calculate whether a bond is part of a conjugated system, the value of N^{conj} in equation (14) is given by the function

$$N_{ij}^{conj} = 1 + \left[\sum_{k(\neq i,j)}^{carbon} f_{ik}^c(r_{ik}) F(X_{ik}) \right]^2 + \left[\sum_{l(\neq i,j)}^{carbon} f_{jl}^c(r_{jl}) F(X_{jl}) \right]^2 \tag{15}$$

where

$$F(x_{ik}) = \begin{cases} 1 & x_{ik} < 2 \\ [1 + \cos(2\pi(x_{ik} - 2))]/2 & 2 < x_{ik} < 3 \\ 0 & x_{ik} > 3 \end{cases} \tag{16}$$

and

$$x_{ik} = N_k^t - f_{ik}^c(r_{ik}). \tag{17}$$

If all of the carbon atoms that are bonded to a pair of carbon atoms i and j have four or more neighbours, equations (15)–(17) yield a value of one for N_{ij}^{conj}, and the bond between these atoms is not considered to be part of a conjugated system. As the coordination numbers of the neighbouring atoms decrease, N_{ij}^{conj} becomes greater than one, indicating a conjugated bonding configuration. Furthermore, the form of equations (15)–(17) distinguishes between different configurations that can lead to conjugation. For example, the value of N^{conj} for a carbon–carbon bond in graphite is nine, while that for a bond in benzene is three. This difference, not included in the first-generation analytic form [1], yields considerable extra flexibility for fitting the energies of conjugated systems. These equations provide a straightforward way of incorporating conjugation effects into a classical potential energy function without having to diagonalize a matrix or go beyond nearest-neighbour interactions. Furthermore, changes in conjugation as bonds break and form are smoothly accounted for. This approach considerably reduces computational time while still including conjugation to a first approximation.

Discrete values for the function defined by equation (14) are chosen to fit the energies of static structures and tricubic splines are used to interpolate between these values. The values for this function are given in table 4.

Table 4. Values at the knots and associated fitting species for the function F_{CC}. All values and derivatives not listed are equal to zero. A continuous function is created using a tricubic spline determined from these values. All derivatives are taken as finite centred divided differences. $F(i, j, k) = F(j, i, k)$, $F(i, j, k > 9) = F(i, j, 9)$, $F(i > 3, j, k) = F(3, j, k)$, and $F(i, j > 3, k) = F(i, 3, k)$.

i	j	k	$F(i, j, k)$	Fitting data/species	i	j	k	$F(i, j, k)$	Fitting data/species
1	1	1	0.105 000	Acetylene	0	1	2	0.009 917 2158	C_3
1	1	2	−0.004 177 5	$H_2C=C=CH$	0	2	1	0.049 397 6637	CCH_2
1	1	3–9	−0.016 085 6	C_4	0	2	2	−0.011 942 669	$CCH(CH_2)$
2	2	1	0.094 449 57	$(CH_3)_2C=C(CH_3)_2$	0	3	1–9	−0.119 798 935	H_3CC
2	2	2	0.022 000 00	Benzene	1	2	1	0.009 649 5698	H_2CCH
2	2	3	0.039 705 87	Average	1	2	2	0.030	$H_2C=C=CH_2$
2	2	4	0.033 088 22	from	1	2	3	−0.0200	C_6H_5
2	2	5	0.026 470 58	difference	1	2	4	−0.023 377 8774	Average from
2	2	6	0.019 852 93	$F(2, 2, 2)$	1	2	5	−0.026 755 7548	$F(1, 2, 3)$ to $F(1, 2, 6)$
2	2	7	0.013 235 29	to	1	2	6–9	−0.030 133 632	Graphite vacancy
2	2	8	0.006 617 64	difference	1	3	2–9	−0.124 836 752	$H_3C–CCH$
2	2	9	0.0	$F(2, 2, 9)$	2	3	1–9	−0.044 709 383	Diamond vacancy
0	1	1	0.043 386 99	C_2H					

Derivatives	Value	Derivatives	Value
$\partial F(2, 1, 1)/\partial i$	−0.052 500	$\partial F(2, 3, 7 − 9)/\partial i$	0.062 418
$\partial F(2, 1, 5 − 9)/\partial i$	−0.054 376	$\partial F(1, 1, 2)/\partial k$	−0.060 543
$\partial F(2, 3, 1)/\partial i$	0.000 00	$\partial F(1, 2, 4)/\partial k$	−0.020 044
$\partial F(2, 3, 2 − 6)/\partial i$	0.062 418	$\partial F(1, 2, 5)/\partial k$	−0.020 044
$\partial F(2, 2, 4 − 8)/\partial k$	−0.006 618		

The term b_{ij}^{DH} in equation (4) is given by

$$b_{ij}^{DH} = T_{ij}(N_i^t, N_j^t, N_{ij}^{conj}) \left[\sum_{k (\neq i, j)} \sum_{l (\neq i, j)} (1 - \cos^2(\Theta_{ijkl})) f_{ik}^c(r_{ik}) f_{jl}^c(r_{jl}) \right] \tag{18}$$

where

$$\Theta_{ijkl} = e_{jik} e_{ijl}. \tag{19}$$

The function $T_{ij}(N_i^t, N_j^t, N_{ij}^{conj})$ is a tricubic spline, and the functions e_{jik} and e_{ijl} are unit vectors in the direction of the cross products $\boldsymbol{R}_{ji} \times \boldsymbol{R}_{ik}$ and $\boldsymbol{R}_{ij} \times \boldsymbol{R}_{jl}$, respectively, where the $\boldsymbol{R}$ are vectors connecting the subscripted atoms. These equations incorporate a standard method for describing forces for rotation about dihedral angles for carbon–carbon double bonds into the analytic bond order. The value of this function is zero for a planar system, and one for angles of 90°. Therefore the function T_{CC} determines the barrier for rotation about these bonds. This function was parametrized such that for carbon–carbon bonds that are not double bonds, this contribution to the bond order is zero. The value for T_{CC} for non-conjugated carbon–carbon bonds was fitted to the barrier for rotation about ethene. The value for T_{CC} for conjugated double bonds was fitted such that for all dihedral angles of 90°, the minimum-energy bond length is 1.45 Å. This value was chosen because it is the average bond length for a hypothetical structure analysed theoretically by Liu *et al* [76]. Like graphite, this structure contains all threefold-coordinated atoms, but with each dihedral angle equal to 90° rather than 0°. The values for the function T_{CC} are given in table 5.

The entire parameter-fitting scheme described above was made considerably easier by assuming only nearest-neighbour interactions. The way to best define this for a continuous

Table 5. Values needed for the carbon–carbon cubic spline T in equation (18). All function values and derivatives not given are equal to zero. Values for $T(i > 3, j, k) = T(3, j, k)$, $T(i, j > 3, k) = T(i, 3, k)$, and $T(i, j, k > 9) = T(i, j, 9)$.

i	j	k	$T(i, j, k)$	Fitting data/structure
2	2	1	$-0.070\,280\,085$	Ethene
2	2	9	$-0.008\,096\,75$	Solid-state structure

function, however, is problematic. The approach used here is the same as that used by Tersoff. The value of $f^c(r)$ is defined by a switching function of the form

$$f_{ij}^c(r) = \begin{cases} 1 & r < D_{ij}^{\min} \\ [1 + \cos((r - D_{ij}^{\min})/(D_{ij}^{\max} - D_{ij}^{\min}))]/2 & D_{ij}^{\min} < r < D_{ij}^{\max} \\ 0 & r > D_{ij}^{\max} \end{cases} \quad (20)$$

where $D_{ij}^{\max} - D_{ij}^{\min}$ defines the distance over which the function goes from one to zero. The problem comes in defining the nearest-neighbour distance. In diamond the nearest-neighbour distance is 1.54 Å, and in graphite the second-neighbour distance is 2.46 Å. To describe both structures, the function must go from one to zero between 1.54 and 2.46 Å. Because this is a rather abrupt cut-off, it is advantageous to maximize the difference between $D^{\max}$ and $D^{\min}$. However, the nearest-neighbour distance in FCC carbon is approximately 2.2 Å, so maximizing this difference with $D_{CC}^{\max} < 2.46$ Å is inconsistent with treating only nearest neighbours in FCC carbon. Because the emphasis of this potential is not high-pressure solid-state structures, parameters are chosen for equation (20) that are consistent with fitting graphite and diamond lattices. These values are given in table 2. Other more complicated schemes will be needed, perhaps including self-consistent bonding concepts, to take advantage of this potential's ability to describe high-pressure solid phases of carbon.

5. Hydrogen

For hydrogen, the potential was fitted to properties of the diatomic molecule, and to features of the potential energy surface for the hydrogen exchange reaction

$$H + H_2 \longrightarrow H_2 + H. \quad (21)$$

The form of the potential is the same as that for carbon, and fitting was performed in several steps. In the first step, the parameters B_{HH2}, B_{HH3}, β_{HH2}, and β_{HH3} in the attractive pair potential (equation (6)) were taken as zero. The remaining parameters in the pair terms together with an analytic value for the bond order for the two near-neighbour bonds in H_3 were fitted to the energy, frequency, and equilibrium distance of the H_2 molecule, and the minimum-energy value (and corresponding bond lengths) for the symmetric stretch of the linear H_3 molecule [77]. The latter energy corresponds to the barrier for the linear exchange reaction equation (21). The resulting pair terms are plotted in figure 4.

After the pair terms were determined, values for the minimum potential energy for the symmetric stretch of H_3 at angles (with respect to a linear molecule at 180°) of 150°, 120°, 90°, and 60° were used to determine analytic values of the bond order at each of these angles. Only the two nearest-neighbour bonds of equal length were considered for the first three angles, while for the last angle the three equal-length bonds were considered. With this approximation only one bond order value is needed for each angle.

In the second fitting step, values for $G_H(\cos(\theta))$ in equation (8) at each of the angles listed above were determined from the bond order values. Unfortunately this led to a
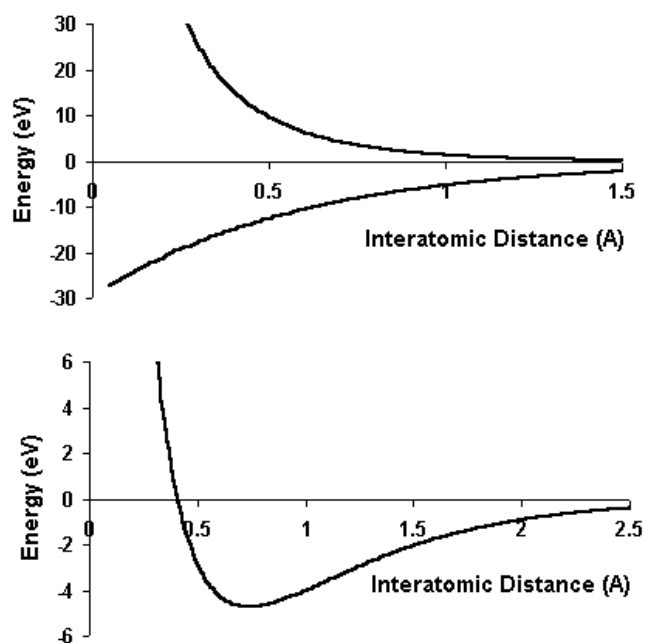
Figure 4. Plots of the pair potentials, equations (5) and (6), for H_2 obtained using the parameters in table 6. Top: the attractive and repulsive pair terms as a function of interatomic distance. Bottom: the sum of the pair terms for the H_2 diatomic molecule.
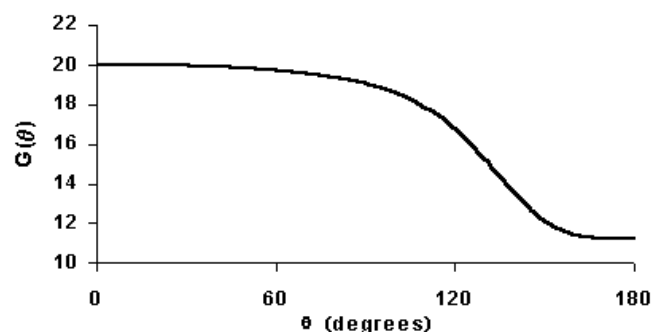

Figure 5. The angular contribution to the bond order equation (8) for hydrogen.

value of $G_H(\cos(\theta = 60°))$ that was lower than the value for $G_H(\cos(\theta = 90°))$. To produce a $G_H(\cos(\theta))$ with a single minimum at $\theta = 180°$, a value for $F_{HH}(1, 1, 1)$ in equation (14) was chosen such that $G_H(\cos(\theta = 60°))$ could be increased to yield a well-behaved angular function. A sixth-order polynomial in $\cos(\theta)$ with coefficients determined by the discrete values of $G_H(\cos(\theta))$ listed in table 6 was used to produce a continuous function for $G_H(\cos(\theta))$. Finally, the parameter λ_{HHH} in equation (8) and parameters in equation (20) were determined to yield a smooth potential energy surface for equation (21) without spurious wells. The resulting angular function is plotted in figure 5, and the parameters associated with a pure hydrogen system are given in table 6.

Table 6. Parameters for the pure hydrogen bond order potential. Values of the functions F and P are equal to zero with the exception listed below. The sixth-order spline representation of the function $G(\cos(\theta))$ can be constructed from the data given.

Pair terms, equations (5) and (6):

$B_1 = 29.632\,593$ eV	$\beta_1 = 1.715\,892\,17$ Å^{-1}	$Q = 0.370\,471\,487\,045$ Å
$B_2 = 0, b_3 = 0$	$A = 32.817\,355\,747$ Å	$\alpha = 3.536\,298\,648$ Å^{-1}
$D_{\min} = 1.1$ Å	$D_{\max} = 1.7$ Å	

Angular function values:

$G(\cos(\theta = 0))$: 19.991 787	$G(\cos(\theta = 90))$: 19.065 124	$G(\cos(\theta = 150))$: 12.164 186
$G(\cos(\theta = 60))$: 19.704 059	$G(\cos(\theta = 120))$: 16.811 574	$G(\cos(\theta = 180))$: 11.235 870

Other parameters:

$\lambda_{\mathrm{HHH}} = 4.0$	$F_{\mathrm{HH}}(1, 1, 1) = 0.249\,831\,916$

Table 7. Parameters for the carbon–hydrogen pair terms, equations (5) and (6).

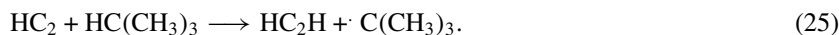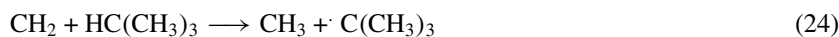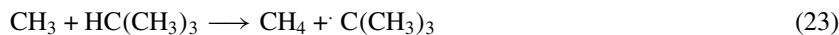|		
$b_1 = 32.355\,186\,6587$ eV	$\beta_1 = 1.434\,458\,059\,25$ Å^{-1}	$Q = 0.340\,775\,728$ Å
$b_2 = 0, b_3 = 0$	$A = 149.940\,987\,23$ eV	$\alpha = 4.102\,549\,83^{-1}$
$D_{\min} = 1.3$	$D_{\max} = 1.8$	

6. Hydrocarbon molecules

Because the angular function $G(\cos(\theta))$ associated with each atomic site has been fitted to pure carbon and pure hydrogen above, only parameters for hydrogen–carbon pair terms and relatively minor modifications to the bond orders are needed to model hydrocarbon molecules. In the first step of parameter fitting, effective pair terms and discrete values of the bond order for carbon–hydrogen bonds were determined. To begin, values for the parameters B_{HH2}, B_{HH3}, β_{HH2}, and β_{HH3} were assumed to be zero, and the value for Q_{CH} was assumed to be the geometric mean of Q_{CC} and Q_{HH}. A guess was used for the initial value of α_{CH1}, and values of A_{CH}, B_{CH1}, and β_{CH1} were fitted to the molecular carbon–hydrogen bond distance and energy in table 1 as well as a value of 2903 cm^{-1} for the stretching vibrational frequency of the tertiary hydrogen in isobutane. Values for the function P_{CH} were then fitted to the appropriate bond energies in ethane and isobutane. Next, values for the parameters λ_{HCH} and λ_{HHC} were fitted to remove spurious wells from the potential surface for the linear hydrogen abstraction reaction

$$\mathrm{H + H\text{–}C(CH_3)_3 \longrightarrow H_2 + {}^{\cdot}C(CH_3)_3.} \tag{22}$$
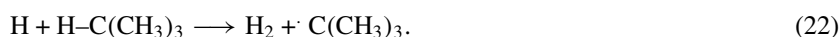
The entire process was iterated until the classical barrier height for the abstraction reaction equation (22) equalled the experimental activation energy of 0.32 eV [78].

In the second step of the fitting process, discrete values of the functions P_{CH} and F_{CH} were systematically fitted to the molecular bond energies listed in table 1. Additional values of the function F_{HC} were then determined by removing spurious wells from the potential energy surfaces for the following (linear) hydrogen migration reactions:

$$\mathrm{CH_3 + HC(CH_3)_3 \longrightarrow CH_4 + {}^{\cdot}C(CH_3)_3} \tag{23}$$

$$\mathrm{CH_2 + HC(CH_3)_3 \longrightarrow CH_3 + {}^{\cdot}C(CH_3)_3} \tag{24}$$

$$\mathrm{HC_2 + HC(CH_3)_3 \longrightarrow HC_2H + {}^{\cdot}C(CH_3)_3.} \tag{25}$$

The resulting values for the parameters and the properties to which they were fitted are given in tables 7–9.

Table 8. Values at the knots and associated fitting species for the function P used in the carbon bond order function. All values and derivatives not listed are equal to zero. A continuous function is created using a bicubic spline determined from these values.

i	j	$P_{CC}(i, j)$	Fitting species	i	j	$P_{CH}(i, j)$	Fitting species
1	1	0.003 026 697 473 481	$(CH_3)HC{=}CH(CH_3)$	1	0	0.209 336 732 825 0380	CH_2
2	0	0.007 860 700 254 745	C_2H_4	2	0	$-0.064 449 615 432 525$	CH_3
3	0	0.016 125 364 564 267	C_2H_6	3	0	$-0.303 927 546 346 162$	CH_4
1	2	0.003 179 530 830 731	i-C_4H_{10}	0	1	0.01	C_2H_2
2	1	0.006 326 248 241 119	c-C_6H_{12}	0	2	$-0.122 042 146 278 2555$	$(CH_3)HC = CH(CH_3)$
				1	1	$-0.125 123 400 628 7090$	C_2H_4
				2	1	$-0.298 905 245 783$	C_2H_6
				0	3	$-0.307 584 705 066$	i-C_4H_{10}
				1	2	$-0.300 529 172 406 7579$	c-C_6H_{12}

Table 9. Values at the knots and associated fitting species for the function F_{CH}. All values and derivatives not listed are equal to zero. A continuous function is created using a tricubic spline determined from these values. $F(i, j, k) = F(j, i, k)$ and $F(i, j, k > 9) = F(i, j, 9)$.

i	j	k	$F_{CH}(i, j, k)$	Fitting species	i	j	k	$F_{CH}(i, j, k)$	Fitting species
0	2	5–9	$-0.009 047 787 516 128 8110$	C_6H_6	1	2	1–9	-0.25	Equations (23)–(25)
1	3	1–9	-0.213	Equations (23)–(25)	1	1	1–9	-0.5	Equations (23)–(25)

7. Predicted properties

As shown above, the formalism adopted here for describing intramolecular bonding is appropriate for both solid-state and molecular systems. The true test of this potential, however, is in its ability to predict properties that are outside of the fitting database. To explore this aspect of the potential, we have calculated a variety of properties of a wide range of molecular and solid-state systems.

A crucial but often neglected first criterion for any potential of this type is to be sure that it gives the intended lowest-energy structure. For this case, the potential should not yield other structures, ordered or not, that are lower in energy than graphite sheets. To test this a molecular dynamics simulation was performed in which a diamond lattice containing 1440 atoms was annealed to above its melting point at constant volume and then cooled back to 0 K. At the end of the simulation, the diamond lattice had converted to a slightly defected graphite sheet. Although not conclusive, this test suggests that graphite is indeed the lowest-energy structure.

One of the goals of this second-generation potential is to produce an improved description of the in-plane elastic properties of graphite and the elastic properties of diamond compared to the previous potentials. Given in table 10 are elastic constants for this potential and Tersoff's carbon potential as well as experimental measurements and results from accurate density functional calculations. This new form yields a reasonable fit to the elastic properties.

A particularly stringent test of a solid-state potential function is the prediction of the energies of defects and surface reconstructions. Given in table 10 are the energies of several defects given by this potential and Tersoff's potential. Also given are estimates for these energies from high-quality total-energy density functional calculations. The new potential yields relative values for the defect energies that are similar to those from first-principles calculations, and are comparable to Tersoff's carbon potential. The improved prediction relative to the first-generation form of this bond order potential is mainly a consequence of the improved fit to the elastic properties.

Table 10. Elastic constants (in Mbar), vacancy formation energies (in eV), and formation energies for interstitial defects (in eV) for diamond.

Property	Tersoff	This work	Experiment/density functional
C_{11}	10.7	10.7	10.8
C_{12}	1.2	1.0	1.3
C_{44}	6.4	6.8	5.8
Vacancy formation	3.4	7.2	7.2[a]
Interstitial (T)	19.6	19.4	23.6[a]
Interstitial (S)	10	12.3	16.7[a]
Interstitial (B)	14.6	11.6	15.8[a]

[a] Density functional results from [89].

Table 11. Energies for various structures of the diamond (111) surface. Energies are in eV/surface atom relative to the bulk-terminated surface.

Structure	Potential I	Potential II	Tersoff	This work	Density functional[a]
Relaxed 1×1	−0.24	−0.24	−0.445	−0.20	−0.37
π-chain	−1.10	−1.03	2.19	−0.77	−0.68
π-molecule	−0.32	−0.25	1.96	0.49	0.28

[a] From [90].

Given in table 11 are the energies for several reconstructions and relaxations for the diamond (111) surface for this potential, our previous potentials, and Tersoff's potential. Also given are estimates from high-quality, total-energy density functional calculations. The lowest-energy structure predicted by the density functional calculations, the π-bonded chain reconstruction, is thought to be responsible for the 2×1 low-energy electron diffraction patterns observed from diamond after chemisorbed hydrogen is removed [79]. This potential predicts that this reconstruction is the most stable of those tested. It also predicts a positive energy relative to the bulk-terminated surface for the π-bonded molecule reconstruction, in agreement with the density functional calculations. The previous-generation potentials produce negative energies for this structure. This is a result of both the improved elastic properties, which destabilize the π-molecule structure due to the high strain energy of this structure, and the improved form for equation (15) over the original effort. The latter allows the bonds in the π-chains to be treated analogously to benzene rather than graphite. This is consistent with simple valence arguments which suggest that these bonds should be 1/2 double and 1/2 single (plus extra stabilization due to electron delocalization) rather than 1/3 double and 2/3 single as in graphite (again with extra stabilization due to electron delocalization) [80].

Tersoff's potential erroneously yields the relaxed bulk-terminated 1×1 structure as the most stable structure. In this case the elastic properties are well described so the surface strain associated with the reconstructions is probably adequate. However, the surface bonds in the π-bonded chain reconstruction are treated like graphite rather than benzene. Furthermore, the back-bonding of the surface radicals on the 1×1 surface is too strong (as suggested by the low vacancy formation energy for diamond), leading to too high a binding energy. The combination of these effects leads to the erroneous ordering of the surface stabilization energies.

The energy change after chemisorbing hydrogen onto the (111) surface is predicted from this potential to be −2.17 and −1.19 eV per surface atom for the relaxed 1×1 and π-bonded chain reconstructed surfaces, respectively, relative to gas-phase H_2 molecules and the relaxed surface. Therefore the relative stability is predicted to change from the reconstructed to the

Table 12. Molecular heats of formation.

Species	Atomization energy (eV)	Zero-point energy (kcal mol^{-1})	ΔH^{pot} (kcal mol^{-1})	ΔH^{expt} (kcal mol^{-1})
CH$_2$	8.4693	11.93	89.86	93.2[a]
CH$_3$	13.3750	19.05	35.48	35.8[a]
Methane	18.1851	26.17	−16.70	−15.99[b]
C$_2$H	11.5722	8.69	133.42	135[a]
Acetylene	17.5651	15.81	53.96	54.33[b]
Ethylene	24.4077	30.05	13.66	14.52[b]
H$_3$C$_2$H$_2$	26.5601	37.17	22.77	28.3[a]
Ethane	30.8457	44.29	−17.31	−16.52[b]
Cyclopropene	28.2589	33.93	98.71	68.3[a]
CH$_2$=C=CH$_2$	30.2392	33.93	53.05	47.4[a]
Propyne	30.3076	33.93	51.47	45.8[a]
Cyclopropane	36.8887	48.17	17.20	16.8[a]
Propene	37.3047	48.17	7.61	8.3[a]
n-C$_3$H$_7$	39.3042	55.29	20.24	25[a]
i-C$_3$H$_7$	39.4601	55.29	16.65	22.2[a]
Propane	43.5891	62.41	−19.82	−19.7[a]
Cyclobutene	42.1801	52.05	69.04	41.5[a]
1, 3-butadiene	43.0035	52.05	50.05	29.8[a]
CH$_3$CH=C=CH$_2$	43.1367	52.05	46.98	42[a]
1-butyne	43.0510	52.05	48.95	42.8[a]
2-butyne	43.0501	52.05	48.97	38[a]
Cyclobutane	49.7304	66.29	12.42	12.7[a]
1-butene	50.0487	66.29	5.08	4.9[a]
cis-butene	50.2017	66.29	1.55	2.3[a]
i-C$_4$H$_9$	52.0451	73.41	17.78	19.4[a]
t-C$_4$H$_9$	52.3778	73.41	10.11	15.2[a]
n-butane	56.3326	80.53	−22.34	−23.5[a]
Isobutane	56.3309	80.53	−22.30	−25.4[a]
1,3-pentadiene	55.9025	70.17	43.95	22.8[a]
1,4-pentadiene	56.5078	70.17	29.99	29.1[a]
Cyclopentene	57.1119	70.17	16.06	13.9[a]
1,2-pentadiene	58.7350	77.29	37.37	38.4[a]
2,3-pentadiene	58.8900	77.29	33.80	36.5[a]
Cyclopentane	63.6443	84.41	−17.09	−10.6[a]
2-pentene	62.9456	84.41	−0.98	−1.1[a]
1-butene, 2-methyl	62.9658	84.41	−1.44	−2[a]
2-butene, 2-methyl	63.1109	84.41	−4.79	−3.2[a]
n-pentane	69.0761	98.65	−24.86	−27.5[a]
Isopentane	69.0739	98.65	−24.81	−28.81[a]
Neopentane	69.0614	98.65	−24.52	−31.3[a]
Benzene	59.3096	59.81	21.75	24[b]
Cyclohexane	76.4606	102.53	−21.29	−20[a]
Naphthalene	93.8784	89.57	37.51	31.04[b]

[a] From 'Computational Chemistry Comparison and Benchmark DataBase', srdata.nist.gov/cccbdb/
[b] From [91].

bulk-terminated surface with hydrogen chemisorption, in agreement with experiments that suggest that this surface of diamond converts from 2×1 to 1×1 upon atomic hydrogen exposure [79]. The change in stability is due to the strain energy present at the reconstructed surface after the chemisorption of hydrogen.

The 2×1 dimer reconstruction on the diamond (001) surface was also examined with this new potential. The bond length for the surface dimer bond is predicted to be 1.37 Å. This is considerably stretched from the double-bond distance of 1.33 Å, reflecting the lattice strain that results from this reconstruction. First-principles, semi-empirical, and other empirical calculations report bond lengths for these strained surface dimer bonds that range from 1.38 Å to greater than 1.58 Å [81–85].

Adding hydrogen to the atoms forming the surface dimers on the reconstructed (001) surface yields a dimer bond length of 1.65 Å. This is considerably stretched from the single-bond length of 1.54 Å for the carbon–carbon bond distance in diamond, and is comparable to the value of 1.67 Å determined from an approximate density functional method [83]. These values again reflect the subsurface strain associated with this surface reconstruction. Attempts to find a minimum-potential-energy structure for the dihydride form of this surface resulted in desorption of the hydrogen, consistent with it being unstable relative to the monohydride/dimer reconstructed surface [79].

Table 12 compares heats of formation at 0 K predicted with this new potential energy function and values derived from experiment for a reasonably extensive set of hydrocarbon molecules that include radicals, saturated, and large unsaturated species. The values estimated from the empirical potential generally agree to less than 15 kcal mol^{-1} with the experimental values. Exceptions occur for the molecules C_4H_2 and ethynyl benzene. For the these two molecules, straightforward analysis of valence structures assuming additive double- and triple-bond strengths suggests that the correct structures should be primarily composed of a triple bond in the π-system, rather than double bonds. The empirical potential, however, is parametrized to produce bonds with significant double-bond character, a structure more appropriate in the limit of long polyethyne chains. This is an example of where the simplified method of describing conjugation described above breaks down.

8. Conclusions

The details of a second-generation reactive empirical bond order potential for hydrocarbons and solid carbon structures have been presented. Changes in the functional forms assumed for the potential together with an expanded fitting database produce a more reliable function for simultaneously predicting bond lengths, energies, and force constants than an earlier version of this potential. An improved fit to the bulk elastic properties of diamond results in better strain energies, and consequently interstitial defect and surface reconstruction energies that compare reasonably well to first-principles predictions.

References

 [1] Brenner D W 1990 *Phys. Rev.* B **42** 9458
 [2] Mowrey R C, Brenner D W, Dunlap B I, Mintmire J W and White C T 1991 *J. Phys. Chem.* **95** 7138
 [3] Garrison B J, Dawnkaski E J, Srivastava D and Brenner D W 1992 *Science* **255** 835
 [4] Williams E R, Jones G C Jr, Fang L, Zare R N, Garrison B J and Brenner D W 1992 *J. Am. Chem. Soc.* **114** 3207
 [5] Alfonso D R, Ulloa S E and Brenner D W 1994 *Phys. Rev.* B **49** 4948
 [6] Taylor R S and Garrison B J 1994 *J. Am. Chem. Soc.* **116** 4465
 [7] Taylor R S and Garrison B J 1995 *Langmuir* **11** 1220
 [8] Brenner D W, Harrison J A, White C T and Colton R J 1991 *Thin Solid Films* **206** 220
 [9] Robertson D H, Brenner D W and Mintmire J W 1992 *Phys. Rev.* B **45** 12 592
[10] Robertson D H, Brenner D W and White C T 1992 *J. Phys. Chem.* **96** 6133
[11] Robertson D H, Brenner D W and White C T 1995 *J. Phys. Chem.* **99** 15 721
[12] Glosli J N and Ree F H 1999 *Phys. Rev. Lett.* **82** 4659
[13] Glosli J N and Ree F H 1999 *J. Chem. Phys.* **110** 441

[14] Harrison J A, Brenner D W, White C T and Colton R J 1991 *Thin Solid Films* **206** 213
[15] Harrison J A, White C T, Colton R J and Brenner D W 1992 *Surf. Sci.* **271** 57
[16] Harrison J A, White C T, Colton R J and Brenner D W 1992 *Phys. Rev.* B **46** 9700
[17] Harrison J A, White C T, Colton R J and Brenner D W 1993 *J. Phys. Chem.* **97** 6573
[18] Harrison J A, White C T, Colton R J and Brenner D W 1993 *Wear* **168** 127
[19] Harrison J A and Brenner D W 1994 *J. Am. Chem. Soc.* **116** 10 399
[20] Perry M D and Harrison J A 1995 *J. Phys. Chem.* **99** 9960
[21] Harrison J A, White C T, Colton R J and Brenner D W 1995 *Thin Solid Films* **260** 205
[22] Perry M D and Harrison J A 1996 *Langmuir* **12** 4552
[23] Perry M D and Harrison J A 1996 *Thin Solid Films* **291** 211
[24] Perry M D and Harrison J A 1997 *J. Phys. Chem.* B **101** 1364
[25] Tutein A B, Stuart S J and Harrison J A 1999 *J. Phys. Chem.* B **103** 11 357
[26] Sinnott S B, Colton R J, White C T and Brenner D W 1994 *Surf. Sci.* **316** L1055
[27] Qi L and Sinnott S B 1997 *J. Phys. Chem.* B **101** 6883
[28] Qi L and Sinnott S B 1998 *J. Vac. Sci. Technol.* A **16** 1293
[29] Qi L and Sinnott S B 1998 *Nucl. Instrum. Methods* B **140** 39
[30] Qi L and Sinnott S B 1998 *Surf. Sci.* **398** 195
[31] Qi L, Young W L and Sinnott S B 1999 *Surf. Sci.* **426** 83
[32] Liu K S S, Yong C W, Garrison B J and Vickerman J C 1999 *J. Phys. Chem.* B **103** 3195
[33] Chatterjee R, Postawa Z, Winograd N and Garrison B J 1999 *J. Phys. Chem.* B **103** 151
[34] Sinnott S B, Qi L F, Shenderova O A and Brenner D W 1999 *Advances in Classical Trajectory Methods: Molecular Dynamics of Clusters, Surfaces, Liquids and Interfaces* vol 4, ed W Hase (Stamford, CT: JAI Press) pp 1–26 ch 1
[35] Wijesundara M B J, Hanley L, Ni B and Sinnott S B 2000 *Proc. Natl Acad. Sci. USA* **97** 23
[36] Harrison J A, Stuart S J, Robertson D H and White C T 1997 *J. Phys. Chem.* B **101** 9682
[37] Garg A, Han J and Sinnott S B 1998 *Phys. Rev. Lett.* **81** 2260
[38] Garg A and Sinnott S B 1998 *Chem. Phys. Lett.* **295** 273
[39] Sinnott S B, Shenderova O A, White C T and Brenner D W 1999 *Carbon* **37** 347
[40] Garg A and Sinnott S B 1999 *Phys. Rev.* B **60** 13 786
[41] Mao Z, Garg A and Sinnott S B 1999 *Nanotechnology* **10** 273
[42] Srivastava D, Brenner D W, Schall J D, Ausman K D, Yu M F and Ruoff R S 1999 *J. Phys. Chem.* B **103** 4330
[43] Brenner D W, Schall J D, Mewkill J P, Shenderova O A and Sinnott S B 1998 *J. Br. Interplanet. Soc.* **51** 137
[44] Tutein A B, Stuart S J and Harrison J A 1999 *J. Phys. Chem.* B **103** 11 357
[45] Shenderova O A, Brenner D W, Nazarov A, Romanov A and Yang L 1998 *Phys. Rev.* B **57** R3181
[46] Shenderova O A, Brenner D W and Yang L H 1999 *Phys. Rev.* B **60** 7043
[47] Shenderova O A and Brenner D W 1999 *Phys. Rev.* B **60** 7053
[48] Shenderova O A, Brenner D W, Omeltchenko A, Su X and Yang L H 2000 *Phys. Rev.* B **61** 3877
[49] Sinnott S B, Colton R J, White C T, Shenderova O A, Brenner D W and Harrison J A 1997 *J. Vac. Sci. Technol.* A **15** 936
[50] Allinger N L, Yuh Y H and Lii J-H 1989 *J. Am. Chem. Soc.* **111** 8551 and references therein
[51] Abell G C 1985 *Phys. Rev.* B **31** 6184
[52] Brenner D W, Shenderova O A and Areshkin D A 1997 Quantum-based analytic interatomic forces and materials simulation *Reviews in Computational Chemistry* ed K B Lipkowitz and D B Boyd (New York: VCH) pp 213–45
[53] Tersoff J 1986 *Phys. Rev. Lett.* **56** 632
[54] Tersoff J 1988 *Phys. Rev.* B **37** 6991
[55] Tersoff J 1988 *Phys. Rev. Lett.* **61** 2879
[56] Tersoff J 1989 *Phys. Rev.* B **39** 5566
[57] Brenner D W 1989 *Mater. Res. Soc. Symp. Proc.* **141** 59
[58] Robertson D H, Brenner D W and White C T 1991 *Phys. Rev. Lett.* **25** 323
[59] Brenner D W, Robertson D H, Elert M L and White C T 1992 *Phys. Rev. Lett.* **70** 1821
[60] Khor K E and Das Sarma A 1988 *Phys. Rev.* B **38** 3318
[61] Kaxiras E and Pandey K C 1988 *Phys. Rev.* B **38** 12 736
[62] Bazant M Z, Kaxiras E and Justo J F 1997 *Phys. Rev.* B **56** 8542
[63] Scheerschmidt C D 1998 *Phys. Rev.* B **58** 4538
[64] Mota F D, Justo J F and Fazzio A 1999 *J. Appl. Phys.* **86** 1843
[65] Alba k and Moller W 1998 *Comput. Mater. Sci.* **10** 111
[66] Dyson A J and Smith P V 1996 *Surf. Sci.* **355** 140

[67] Dyson A J and Smith P V 1997 *Surf. Sci.* **375** 45
[68] Murty M V R and Atwater H A 1995 *Phys. Rev.* B **51** 4889
[69] Beardmore K and Smith R 1996 *Phil. Mag.* A **74** 1439
[70] Che J, Cagin T and Goddard W H 1999 *Theor. Chem. Acc.* **102** 346
[71] Stuart S J, Tutein A B and Harrison J A 2000 *J. Chem. Phys.* **112** 6472
[72] Pettifor D G 1989 *Phys. Rev. Lett.* **63** 2480
[73] Pettifor D G and Oleinik I I 1999 *Phys. Rev.* B **59** 8487
[74] Pettifor D G and Oleinik I I 1999 *Phys. Rev.* B **59** 8500
[75] Chelikowski J R and Chou M Y 1998 *Phys. Rev.* B **37** 6504
[76] Liu A Y, Cohen M L, Hass K C and Tamor M A 1991 *Phys. Rev.* B **43** 6742
[77] Liu B and Seigbahn P 1978 *J. Chem. Phys.* **58** 2457
[78] Page M and Brenner D W 1991 *J. Am. Chem. Soc.* **113** 3270
[79] Kubiak G D and Kolasinski K W 1989 *Phys. Rev.* B **39** 1381 and references therein
[80] Pauling L 1960 *The Nature of the Chemical Bond* (Ithaca, NY: Cornell University Press)
[81] Zing Z and Whitten J L 1994 *Phys. Rev.* B 50 2598
[82] Frauenheim T, Stephan U, Blaudeck P, Porezag D, Busmann H G, Zimmermannedling W and Lauer S 1993
          Phys. Rev. B **48** 18 189
[83] Mehandru S P and Anderson A B 1991 *Surf. Sci.* **248** 369
[84] Skokov S, Carmer C S, Weiner B and Frenklach M 1994 *Phys. Rev.* B **49** 5662
[85] Furthmuller J, Hafner J and Kresse G 1996 *Phys. Rev.* B **53** 7334
[86] Lewis G N and M Randall 1961 *Thermodynamics* (New York: McGraw-Hill) appendix A7-8, p 682
[87] Yin and Cohen 1983 *Phys. Rev. Lett.* **50** 2006
          Yin and Cohen 1983 *Phys. Rev.* B **29** 6996
[88] Harrison W A 1983 *Phys. Rev.* B **27** 3592
[89] Bernholc J, Antonelli A, Del Sole T M, Bar-Yam Y and Pantelides S T 1989 *Phys. Rev. Lett.* **61** 2689
[90] Vanderbilt D and Louie S G 1984 *Phys. Rev.* B **30** 6118
[91] Lewis G N and Randall M 1961 *Thermodynamics* 2nd edn (New York: McGraw-Hill)